

*Енергопоглинаюча здатність може бути використана для вимірювання опору матеріалу балістичному удару. Метою даної роботи є аналіз енергопоглинаючої пластини з гумовим покриттям за допомогою пострілу деформованими снарядами. Дане дослідження проведено з використанням чисельного моделювання на основі кінцевого елемента, підтвердженого експериментальними результатами. Установка моделювання на сталевій пластині з різною твердістю з додаванням товщини гуми виготовлена у вигляді балістичної випробувальної панелі. Шари не були закріплені на задній пластині. Постріл в панель здійснювався з використанням деформованої кулі калібру 5,56×45 мм з відстанню 15 м від нормального кута атаки. Для моделювання використовувався алгоритм по методу кінцевих елементів з моделями еластопластичного матеріалу Джонсона-Кука і Муні-Рівлін. Результати моделювання показують, що енергія балістичного удару, отримана і поглинена панеллю, значно зростає незабаром після зіткнення до тих пір, поки не досягне певного значення на одній пластині, де енергія зменшиться завдяки успішному проникненню снаряда в пластину. У той час як на шаруватій пластині, після того, як снаряду вдалося проникнути в передню бічну пластину, енергія поглинання досягла максимального значення і не змінилася, що призвело до того, що снаряд не зміг проникнути в наступний шар. Дані результати свідчать про те, що додавання гуми з шаруватою структурою дозволяє поглинати енергію балістичного удару.*

*Ключові слова: поглинач енергії, тверда пластина, м'яка пластина, балістична шарувата пластина, гума, балістичний удар, моделювання*

UDC 621

DOI: 10.15587/1729-4061.2018.127345

# ENERGY ABSORBERS ON THE STEEL PLATE – RUBBER LAMINATE AFTER DEFORMABLE PROJECTILE IMPACT

**Helmy Purwanto**

Department of Mechanical Engineering  
Wahid Hasyim University  
Jalan. Menoreh Tengah, X/22,  
Sampangan, Semarang, Indonesia, 50236  
Doctoral Student\*

Email: helmypurwanto@unwahas.ac.id

**Rudy Soenoko**

Doctor of Mechanical Engineering, Professor\*  
Email: rudysoen@ub.ac.id

**Anindito Purnowidodo**

Doctor of Mechanical Engineering,  
Associate Professor\*

Email: anindito@ub.ac.id

**Agus Suprpto**

Doctor of Mechanical Engineering, Professor  
Department of Mechanical Engineering  
University of Merdeka Malang  
Jalan. Terusan Raya Dieng, 62-64,  
Malang, Indonesia, 65146

Email: agussuprpto@yahoo.com

\*Department of Mechanical Engineering  
Brawijaya University Malang

Jalan. Mayjend Haryono, 167, Malang, Indonesia, 65145

## 1. Introduction

Defense and security play an important role in state sovereignty. One of the most common defense equipment used in the military world is combat vehicles. Combat vehicles are special vehicles equipped with combat equipment and must be able to withstand the opponent's attacks. The success of combat vehicles is in the completion of defense and defense missions [1].

The material on combat vehicles in general is a steel plate. Steel is used because it has characteristics that can be strengthened, easily shaped and can form a structure. Steel is easily made and also has the nature of protection against ballistics. Ballistics is the study of the acceleration of moving objects, in modern ballistics science it is further defined as the study of the force, motion and impact of a projectile fired

from a weapon [2]. Projectile clash with the plate resulted in a very high strain on the narrow area [3].

Ballistic resistance is not only influenced by target violence. Ballistic resistance is a complex function of hardness, toughness, tensile strength, tenacity and yield strength [4]. High impact energy absorption is one of the performances of ballistic resistant materials [5]. So do layered manufacturing of some materials to combine these properties. Rubber is one of the elastic materials that can absorb impact energy. Damage caused by ballistics is one of the causes of the inability to absorb impact energy between the panel and projectile. The coating of elastomers [6] and polyurea [7] on metals can enhance ballistic resistance.

Ballistic impact parameters are complex, such as the relative speed of projectiles and targets, projectile and target shapes, relative stiffness and projectile mass and targets,

contact surfaces, geometry and boundary conditions and projectile material characteristics and targets [8] and environmental factors such as speed and direction of wind, if testing is done outdoors. Hence, the resulting failure is very complex. It takes deep observation and analysis and focuses on knowing every difference from the experiment.

Using a physical model in an experiment requires a lot of experimentation that takes a long time and is quite costly. Technological advances to avoid the number of experiments are offered using numerical simulations [8, 10].

In the test experiment sometimes no data obtained detail and desired. The numerical simulation of selected models can obtain detailed and comprehensive data and results [11]. The simulation results should be certified by using test experiments to obtain accuracy. A good correlation between the simulation using the commercial code and the experimental method was obtained on thin laminate composites with Kevlar 29 reinforcement [8].

---

## 2. Literature review and problem statement

---

Preparation of layered panels, each layer has its own function, the main function of the front layer is to absorb the kinetic energy of the bullet, balancer, deflection and deformation, while the next layer of the plate serves to absorb the remaining energy of kinetic and shrapnel [12]. The first layer of sanitary composite armor is made with the aim of collecting and breaking the projectile while the next layer and the back-plate function to absorb the remaining kinetic energy from the projectile to stop its speed [13].

The weight and shape of the projectile tip affect the impact of ballistics. The simulation results found that the double layer was able to increase the ballistic resistance of 8.0–25.0 % for the shape of the flat bullet tip, compared with single plates of the same weight. While the impact of projectiles for conical tip projectiles is almost the same on double plates as well as single plates [14]. In contrast to [15], single plate has superior performance compared to multilayer plate.

The simulation shows that projectile nose shape independently affects minimum ballistic limit [16]. The blunt end of the projectile project increases the ballistic limit on the double plate, but falls when using the ends of the ogival projectile. With the simulations proved, the greater the projectile durability of ballistic resistance increased on the monolithic plate compared to the aluminum-coated plate and the projectile size was more influential than the target configuration variation [17].

Using numerical analysis, the addition of polyuria is capable of absorbing projectile impact energy [7] and contributes positively to the reduction in the residual velocities of projectiles fired on layered composites [18]. The thicker the ceramic layer on the ramp plate, with simulations and ballistic resistance experiments increasing [19]. Ballistic resistance increased with the addition of an epoxy adhesive to the ceramics [20]. Polymer composites are used in sandwich form because they are capable of inhibiting projectiles by reducing kinetic energy due to ballistic impact [21].

The process of bullet penetration and evaluation of the energy changes that occur during projectile collisions is done with finite element software. Panels with alumina layer Ti<sub>6</sub>Al<sub>4</sub>V, UHMPE and as back-plate were varied using Ti6Al4V material, carbon fiber plate and aluminum alloy. 60 % pro-

jectile energy was transferred to the alumina. Back plate Ti<sub>6</sub>Al<sub>4</sub>V provides the best resilience compared to carbon fiber plate and aluminum alloy as it improves the energy balance in UHMPE middle layer [22]. The ballistic impact resistance and impact energy absorption of the hybrid composite laminates were enhanced by deposition of micro and nano-fillers into the surface of the Kevlar fibers fabrics [23].

Ballistic resistance is affected by material and manufacturing properties. Ballistic resistance of a ballistic resistant material can be observed from damage caused by projectile impacts called ballistic effects. This ballistic impact is influenced by the ability of the material panel to absorb the impact energy. The layered manufacturing produces a different impact with a single plate. Rubber has an elastic material capable of reducing the impact. This study is focused on panel manufacturing independent (non-fix) of the black plate. This manufacturing has not been much of a focus on previous research. The effect of layered plate manufacturing is made independent of one another through the addition of rubber to its ballistic capability in terms of energy absorbed by projectile impact.

---

## 3. The aim and objectives of the study

---

The aim of this study is to determine and analyze the energy absorbed on a single plate and a layered plate with a rubber damper due to deformable projectile shot by using finite element numeric simulation.

To accomplish the set aim, the following tasks were set:

- selection of material model and simulation and verification with the experimental test result;
- analyze the results of the simulation in various variables to determine the influence.

---

## 4. Material, methods and numerical model of research

---

In this study, the materials used as test experiments for validation are commercial steel plate (soft plate/back plate), hard plate and commercial rubber. Each of these materials has properties as shown in Table 1. Model of steel plate and projectile uses Johnson-Cook strength equation (1) [24], while rubber uses Mooney-Rivlin equation (2) [24–26]. Material data for simulation is shown in Table 2.

Plasticity of metal plate uses Johnson Cook Strength equation;

$$\sigma_{eq} = (A + B\epsilon^N)(1 + C \ln \epsilon^*) \left( 1 - \left( \frac{T - T_0}{T_{melt} - T_0} \right)^M \right), \quad (1)$$

with  $\sigma_{eq}$  is the equivalent stress (MPa),  $A$  is the yield stress constant (MPa),  $B$  is the hardening constant (MPa),  $\epsilon$  is the equivalent strain,  $C$  is the strain rate constant,  $N$  is the hardening exponent,  $M$  is the thermal softening exponent,  $\epsilon^*$  is the plastic strain rate and  $T_{melt}$  is the melting temperature of the material (K). While hyperelastic rubber uses Mooney-Rivlin equation;

$$\sigma = 2C_1 \left[ D - \frac{1}{D^3} \right] + 2C_2 \left[ 1 - \frac{1}{D^3} \right], \quad (2)$$

with  $\sigma$  being the equivalent stress (MPa),  $C_1$  and  $C_2$  are probability constants (MPa) and  $D$  is the extension ratio (MPa).

The simulation design is shown in Fig. 1 and meshing 0.1 mm is shown in Fig. 2. The speed of the projectile is set at 989 m/s, the time before the start of the collision until the end of the program is  $1.5 \times 10^{-4}$  seconds. While the test scheme corresponds to Fig. 3, the research variables are shown in Table 3. The total energy absorbed is obtained by regulating the solution data of total energy received on the panel.

Table 1

The average mechanical properties of materials

Material	Hardness	Max Stress (MPa)	(%)	Impact Energy (J)	Tear strength (N/mm)	Determination of compressions (%)
Soft plate/back plate	118.21 BHN	458.16	31	62.48	–	–
Hard plate	478.23 BHN	1466.19	13	47.77	–	–
Rubber	67 Shore A	4.21	120	–	2.08	34.01

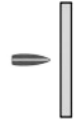





Table 2

Material data for steel plate [27] and data for rubber materials [25]

Data Material	Lead	Brass	Soft Plate	Hard Plate	Rubber
Density $\rho$ (kg/m <sup>3</sup> )	10,660	8,520	8859.782	9112.439	1,000
Young's modulus E (MPa)	1,000	115,000	200,000	210,000	–
Poisson's ratio $\nu$	0.42	0.31	0.3	0.33	–
Specific heat $C_p$ (J/kgK)	124	385	486	452	–
Initial Yield Stress A (MPa)	24	206	146.7	819	–
Hardening Constant B (MPa)	300	505	896.9	308	–
Hardening Exponent N	1	0.42	0.32	0.64	–
Strain Rate Constant C	0.1	0.01	0.033	0.0098	–
Thermal Softening Exponent M	1	1.68	0.323	1	–
Melting Temperature $T_{melt}$ (K)	760	1,189	1,773	1,800	–
Material constant C10 (MPa)	–	–	–	–	150
Material constant C01 (MPa)	–	–	–	–	1.5

Table 3

Sandwich plate configurations

Configuration	Geometry	Thickness	Code
Soft plate		6 mm soft plate	S
Soft-soft plate		6 mm soft plate – 6 mm back plate	S.0
Soft-rubber-soft plate		6 mm soft plate – 2 mm rubber – 6 mm back plate	S.2
		6 mm soft plate – 4 mm rubber – 6 mm back plate	S.4
		6 mm soft plate – 6 mm rubber – 6 mm back plate	S.6
Hard plate		6 mm hard plate	H
Hard-soft plate		6 mm hard plate – 6 mm back plate	H.0
Hard-rubber-soft plate		6 mm hard plate – 2 mm rubber – 6 mm back plate	H.2
		6 mm hard plate – 4 mm rubber – 6 mm back plate	H.4
		6 mm hard plate – 6 mm rubber – 6 mm back plate	H.6

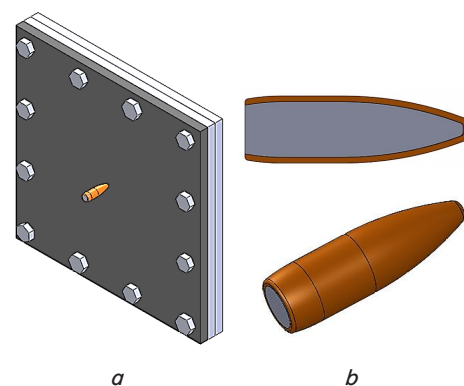


Fig. 1. Design simulation: a – panel target; b – projectile

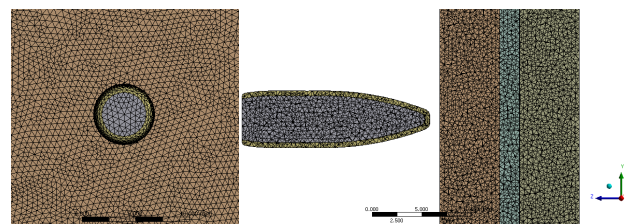


Fig. 2. Meshing concretize

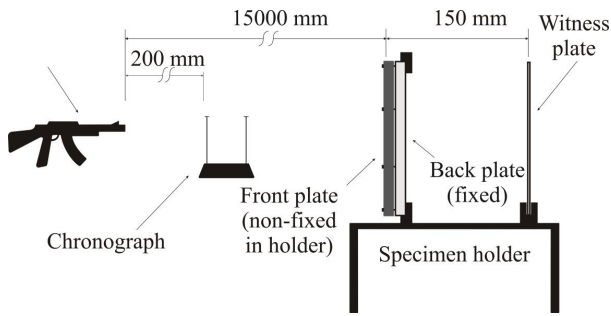


Fig. 3. Experimental testing scheme and conditioning in the simulation

### 5. Validation simulation

Multiple test experiments were performed to validate numerical simulations. This is done to see the similarity of ballistic impact on experiment and simulation. The result of experimental and simulated ballistic effects is shown in Fig. 4.

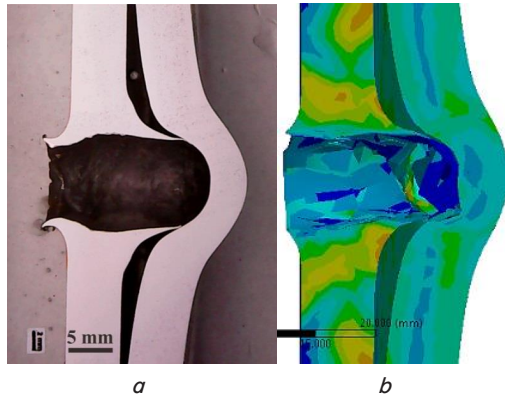


Fig. 4. Ballistic test result: *a* – experiment; *b* – simulations

From Fig. 4, dimensions of ballistic impact on the experiment and simulation are measured. From the measurement results obtained, the level of similarity of ballistic impact is 93 % or with an error of 7 %.

### 6. The result of the absorbers energy

The result of the numerical simulation is obtained the total energy absorbed at the time of stopping in each configuration. The energy absorbed by each configuration for a given time is  $1.5 \times 10^{-4}$  seconds as shown in Fig. 5.

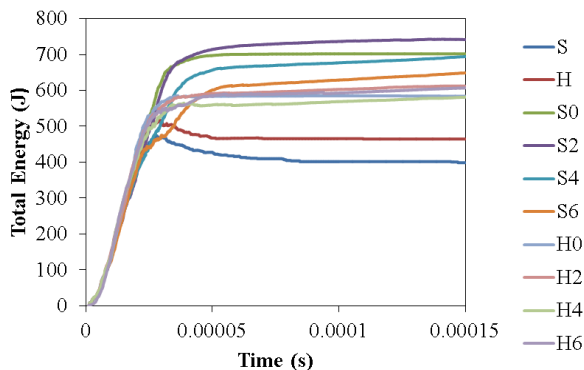


Fig. 5. Total energy versus time

Energy absorbed rises shortly after a collision between projectiles and panels. The process of energy absorption on a single plate increases until the maximum number and decreases in a constant manner. In the S configuration, energy rises significantly until it reaches a maximum of 473.70 J and occurs in  $3.10 \times 10^{-5}$  seconds. After achieving the maximum amount of energy absorbed, the energy decrease occurs at  $6.38 \times 10^{-5}$  seconds and constantly does to 410.66 J until the simulation is terminated.

Similar to the S configuration, in the H configuration the energy absorption rises significantly to a maximum of 518.53 J and occurs in  $2.25 \times 10^{-5}$  seconds. After reaching the maximum energy level, it drops to 464.48 J in  $5.90 \times 10^{-5}$  seconds and then tends to be constant until the simulation is terminated.

Energy absorption on layered plates tends to be different from single plates. The amount of energy rises significantly shortly after a collision to a certain point and becomes stable until the simulation is terminated. The average energy absorbed in the layered plated plate configuration is faster than the single plate configuration.

The energy absorption capability of each configuration is different. The greatest energy absorbed by each configuration is shown in Fig. 6.

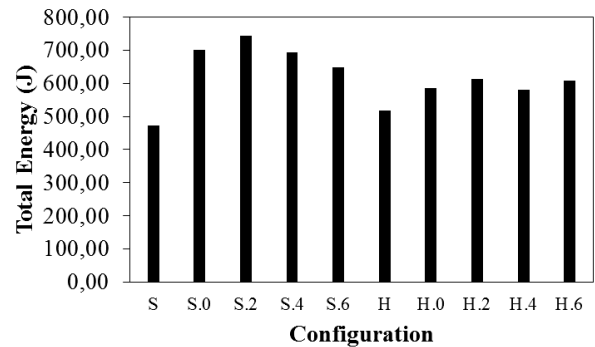


Fig. 6. Total energy versus configuration

The energy absorption on a single plate between the soft plate (S) is smaller than the hard plate (H). However, for layered-plate configurations the average high energy absorption occurs on the plate using the soft configuration. The greatest energy occurs in the S2 configuration on the soft-rubber-soft plate panel with the addition of 2 mm thick rubber. The same is true for the hard configuration plate, where the highest total absorbed energy in the H2 configuration was achieved through adding 2 mm of rubber.

Fig. 7 shows the equivalent stress when the energy reaches the maximum value and the stable value after the maximum in the S configuration. Fig. 8 shows the same conditions in the H-configuration and Fig. 9 shows equivalent stress on the S2 and H2 configuration plates. The color of the simulation results shows the distribution of the received voltage of the plate due to the projectile impact force. Red color shows higher concentration of force while blue color shows lower concentration of force.

Fig. 10 shows the end simulation results on the plated plates S2, S4 and S6 configurations. Visible addition of rubber thickness between plates causes increased equivalent stress on the back plate.

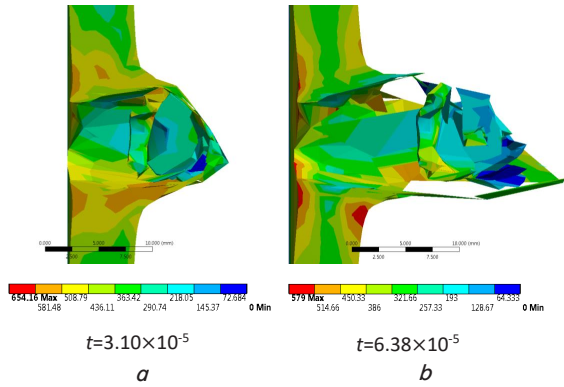


Fig. 7. Equivalent stress on a single configuration plate S: *a* – when the maximum absorption energy is reached; *b* – the absorption energy stabilizes

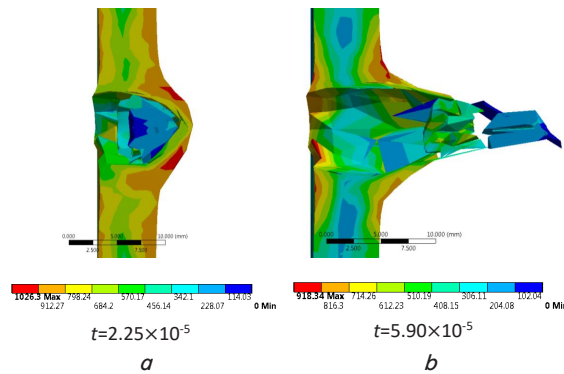


Fig. 8. Equivalent stress on a single configuration plate H: *a* – when the maximum absorption energy is reached; *b* – the absorption energy stabilizes

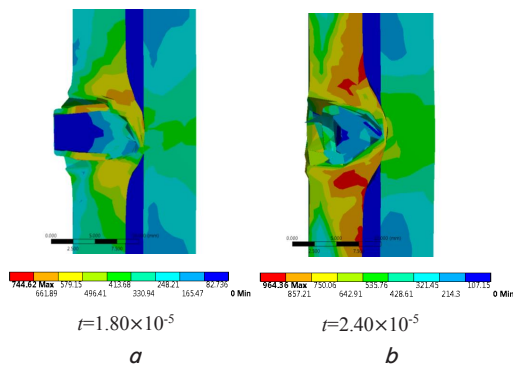


Fig. 9. Equivalent stress on layered plates when maximum absorption energy is reached: *a* – S2 configuration; *b* – H2 configuration

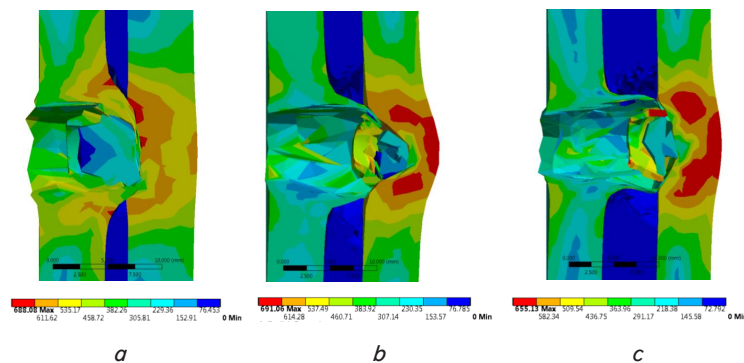


Fig. 10. Equivalent stress on layered plates end of simulation  $t=4.8001 \times 10^{-5}$ : *a* – S2 configuration; *b* – S4 configuration and *c* – S6 configuration

### 7. Discussion of the absorbers energy

The maximum energy absorption on a single configuration plate S occurs at approximately seconds to  $3.1 \times 10^{-5}$ . And after reaching that time, the energy absorption decreased. This is because at that moment the projectile has penetrated the plate in a single configuration as shown in Fig. 7. The impact of a large projectile cannot hold the panel so that the panel reaches its maximum voltage and the panel is pierced after a second to  $6.38 \times 10^{-5}$ . After the seconds and the projectiles have passed through the panel, the remaining energy is proved by the tension still visible on the plate (Fig. 7, *b*).

This is also the case with a single H configuration plate. The maximum energy occurs just before the projectile passes through the plate as shown in Fig. 8*a*. This process occurs in seconds to  $2.25 \times 10^{-5}$ . Also visible voltage on the plate reaches the maximum around the impact of the projectile. The energy decreases and is relatively stable after  $5.90 \times 10^{-5}$  seconds, this occurs after the projectile passes through the plate as shown in Fig. 8, *b*.

In contrast to the plated plates, energy rises significantly shortly after the projectiles consume the panel until it reaches a certain number and then tends to be constant. This boundary mark with a perverted projectile will pierce the front plate in a layered configuration. In the S2 configuration panel, this condition occurs at  $1.80 \times 10^{-5}$  seconds as shown in Fig. 9, *a*, as seen from the projectile condition will penetrate the front plate.

In H2 configuration, the process occurs similarly to the S2 configuration. Energy rises significantly shortly after the projectile strikes the plate up to a certain value. The limit of increase until it reaches the energy that tends to constant occurs in seconds to  $2.40 \times 10^{-5}$ . This condition occurs when the projectile is capable of piercing the front plate in the H2 configuration as shown in Fig. 9, *b*.

The larger S2 configuration absorbs the impact energy of the bullet (Fig. 6), this is because the S configuration consists of soft-rubber plates and soft plates. The soft plate energy impeller is larger than the hard plate (Table 1) in the H configuration, the addition of rubber thickness increased to 6 mm actually weakens the layered plate structure which causes the total energy to decrease compared to rubber thickness of 2 mm.

The addition of rubber to the layered plate arrangement can improve the absorption of ballistic impact energy. The rubber between the plates can absorb the collision energy of the plate, so that the impact energy is not directly forwarded to the next layer of the plate. This is because rubber is an elastic material and has good energy absorption.

However, the addition of thickness to 4 mm and 6 mm of rubber precisely absorption of energy collisions decreased. This is because rubber has non-rigid properties and is not resistant to penetration. The addition of rubber thickness between the two plates causes an increase in weak space so that the first plate fragments and the projectiles penetrating the first plate stronger push the back plate. This shows the equivalent stress on the back plate at the end of the simulation as shown in Fig. 10. So that the optimum energy absorption on the addition of rubber with a thickness of 2 mm, both in soft plate configuration (S configurations) and hard plate (H configurations).

Type of rubber can affect the energy absorption, because each type of rubber has different elasticity properties. The selection of rubber types in this study is not a concern, so the effectiveness of energy absorption by rubber cannot be analyzed further. The bolt tightening system in panel making can also be varied, because the bolt system makes the impact vibration propagation different. With the addition of increasingly complex boundary conditions, the simulation will get more complete data but require long

simulation calculations and requires a computer with higher specifications.

---

## 8. Conclusions

---

1. Experimental and simulation results of ballistic impact tests look similar. The level of similarity of ballistic impact is 93 % or with an error of 7 %.

2. Energy due to the impact ballistic received and absorbed on the panel rises significantly shortly after the collision. On a single plate, this occurs until it reaches a certain number, then the energy will decrease because the projectile succeeded in penetrating the plate. While on the layered plate, after the projectile successfully penetrates the front side plate, absorption energy reaches the maximum number and then remains constant until the end of the simulation, which caused the projectile to be unable to penetrate the next plate layer. And optimal absorption of energy by plate occurs in the addition of 2 mm of rubber either on a soft plate or hard plate layer.

---

## References

1. Application of Lightweighting Technology to Military Aircraft, Vessels, and Vehicles / Brinson L. C., Allison J., Chen J., Clarke D. R. et. al. National Academy Press, Washington, DC, 2012.
2. Effect of target thickness in blunt projectile penetration of Weldox 460 E steel plates / Børvik T., Hopperstad O. S., Langseth M., Malo K. A. // *International Journal of Impact Engineering*. 2003. Vol. 28, Issue 4. P. 413–464. doi: [https://doi.org/10.1016/s0734-743x\(02\)00072-6](https://doi.org/10.1016/s0734-743x(02)00072-6)
3. Zukas J. A. Impact dynamics: theory and experiment. DTIC Document, 1980. 66 p.
4. Effect of heat treatment on mechanical and ballistic properties of a high strength armour steel / Jena P. K., Mishra B., Ramesh Babu M., Babu A., Singh A. K., SivaKumar K., Bhat T. B. // *International Journal of Impact Engineering*. 2010. Vol. 37, Issue 3. P. 242–249. doi: <https://doi.org/10.1016/j.ijimpeng.2009.09.003>
5. Jacobs M. J. N., Van Dingenen J. L. J. Ballistic Protection Mechanisms in Personal Armour // *Journal of Materials Science*. 2001. Vol. 36, Issue 13. P. 3137–3142. doi: <https://doi.org/10.1023/a:1017922000090>
6. Factors influencing the ballistic impact resistance of elastomer-coated metal substrates / Roland C. M., Fragiadakis D., Gamache R. M., Casalini R. // *Philosophical Magazine*. 2013. Vol. 93, Issue 5. P. 468–477. doi: <https://doi.org/10.1080/14786435.2012.722235>
7. Polyurea coated composite aluminium plates subjected to high velocity projectile impact / Mohotti D., Ngo T., Mendis P., Raman S. N. // *Materials & Design (1980-2015)*. 2013. Vol. 52. P. 1–16. doi: <https://doi.org/10.1016/j.matdes.2013.05.060>
8. Silva M. A. G., Cismaşiu C., Chiorean C. G. Numerical simulation of ballistic impact on composite laminates // *International Journal of Impact Engineering*. 2005. Vol. 31, Issue 3. P. 289–306. doi: <https://doi.org/10.1016/j.ijimpeng.2004.01.011>
9. Choi H. Y., Downs R. J., Chang F.-K. A New Approach toward Understanding Damage Mechanisms and Mechanics of Laminated Composites Due to Low-Velocity Impact: Part I—Experiments // *Journal of Composite Materials*. 1991. Vol. 25, Issue 8. P. 992–1011. doi: <https://doi.org/10.1177/002199839102500803>
10. Choi, H. Y., Wu, H.-Y. T., Chang, F.-K. A New Approach toward Understanding Damage Mechanisms and Mechanics of Laminated Composites Due to Low-Velocity Impact: Part II—Analysis // *Journal of Composite Materials*. 1991. Vol. 25, Issue 8. P. 1012–1038. doi: <https://doi.org/10.1177/002199839102500804>
11. Ballistic and numerical simulation of impacting goods on conveyor belt rubber / Molnar W., Nugent S., Lindroos M., Apostol M., Varga M. // *Polymer Testing*. 2015. Vol. 42. P. 1–7. doi: <https://doi.org/10.1016/j.polymertesting.2014.12.001>
12. Šháněl V., Španiel M. Ballistic Impact Experiments and Modelling of Sandwich Armor for Numerical Simulations // *Procedia Engineering*. 2014. Vol. 79. P. 230–237. doi: <https://doi.org/10.1016/j.proeng.2014.06.336>
13. An energy-based model for ballistic impact analysis of ceramic-composite armors / Naik N., Kumar S., Ratnaveer D., Joshi M., Akella K. // *International Journal of Damage Mechanics*. 2012. Vol. 22, Issue 2. P. 145–187. doi: <https://doi.org/10.1177/1056789511435346>
14. Protection performance of double-layered metal shields against projectile impact / Teng X., Dey S., Børvik T., Wierzbicki T. // *Journal of Mechanics of Materials and Structures*. 2007. Vol. 2, Issue 7. P. 1309–1329. doi: <https://doi.org/10.2140/jomms.2007.2.1309>
15. Flores-Johnson E. A., Saleh M., Edwards L. Ballistic performance of multi-layered metallic plates impacted by a 7.62-mm APM2 projectile // *International Journal of Impact Engineering*. 2011. Vol. 38, Issue 12. P. 1022–1032. doi: <https://doi.org/10.1016/j.ijimpeng.2011.08.005>

16. On the ballistic resistance of double-layered steel plates: An experimental and numerical investigation / Dey S., Børvik T., Teng X., Wierzbicki T., Hopperstad O. S. // *International Journal of Solids and Structures*. 2007. Vol. 44, Issue 20. P. 6701–6723. doi: <https://doi.org/10.1016/j.ijsolstr.2007.03.005>
17. Senthil K., Iqbal M. A. Effect of projectile diameter on ballistic resistance and failure mechanism of single and layered aluminium plates // *Theoretical and Applied Fracture Mechanics*. 2013. Vol. 67-68. P. 53–64. doi: <https://doi.org/10.1016/j.tafmec.2013.12.010>
18. Analytical and numerical investigation of polyurea layered aluminium plates subjected to high velocity projectile impact / Mohotti D., Ngo T., Raman S. N., Mendis P. // *Materials & Design*. 2015. Vol. 82. P. 1–17. doi: <https://doi.org/10.1016/j.matdes.2015.05.036>
19. A Development of Integral Composite Structure for the Ramp of Infantry Fighting Vehicle / Lee C. H., Kim C. W., Yang S. U., Ku B. M. // *23rd International Symposium on Ballistics*. Tarragona, 2007. P. 895.
20. The effect of the thickness of the adhesive layer on the ballistic limit of ceramic/metal armours. An experimental and numerical study / López-Puente J., Arias A., Zaera R., Navarro C. // *International Journal of Impact Engineering*. 2005. Vol. 32, Issue 1-4. P. 321–336. doi: <https://doi.org/10.1016/j.ijimpeng.2005.07.014>
21. Modelling of the energy absorption by polymer composites upon ballistic impact / Morye S. S., Hine P. J., Duckett R. A., Carr D. J., Ward I. M. // *Composites Science and Technology*. 2000. Vol. 60, Issue 14. P. 2631–2642. doi: [https://doi.org/10.1016/S0266-3538\(00\)00139-1](https://doi.org/10.1016/S0266-3538(00)00139-1)
22. Design and ballistic penetration of the ceramic composite armor / Liu W., Chen Z., Cheng X., Wang Y., Amankwa A. R., Xu J. // *Composites Part B: Engineering*. 2016. Vol. 84. P. 33–40. doi: <https://doi.org/10.1016/j.compositesb.2015.08.071>
23. Haro E. E., Odeshi A. G., Szpunar J. A. The energy absorption behavior of hybrid composite laminates containing nano-fillers under ballistic impact // *International Journal of Impact Engineering*. 2016. Vol. 96. P. 11–22. doi: <https://doi.org/10.1016/j.ijimpeng.2016.05.012>
24. Johnson G. R., Cook W. H. A Constitutive Model and Data for Metals Subjected to Large Strains, High Strain Rates, and High Temperatures // *Proceedings 7th International Symposium on Ballistics*. 1983. P. 541–547.
25. Treloar L. R. G. Stress-strain data for vulcanised rubber under various types of deformation // *Transactions of the Faraday Society*. 1944. Vol. 40. P. 59. doi: <https://doi.org/10.5254/1.3546701>
26. Guo Z., Sluys L. J. Constitutive modelling of hyperelastic rubber-like materials // *Heron*. 2008. Vol. 53, Issue 3. P. 109–132.
27. Børvik T., Dey S., Clausen A. H. Perforation resistance of five different high-strength steel plates subjected to small-arms projectiles // *International Journal of Impact Engineering*. 2009. Vol. 36, Issue 7. P. 948–964. doi: <https://doi.org/10.1016/j.ijimpeng.2008.12.003>